

Shock geometry and physics in the supernova remnant SNR 0509-67.5



*sknezevic@aob.rs

Sladjana Knežević^{1*}, Rino Bandiera², Giovanni Morlino², Steve Schulze³,
John C. Raymond⁴, Glenn van de Ven⁵



¹ Astronomical Observatory of Belgrade, Serbia; ² INAF/Observatorio Astrofisico di Arcetri, Firenze, Italy;

³ Center for Interdisciplinary Exploration and Research in Astrophysics (CIERA), Northwestern University, USA;

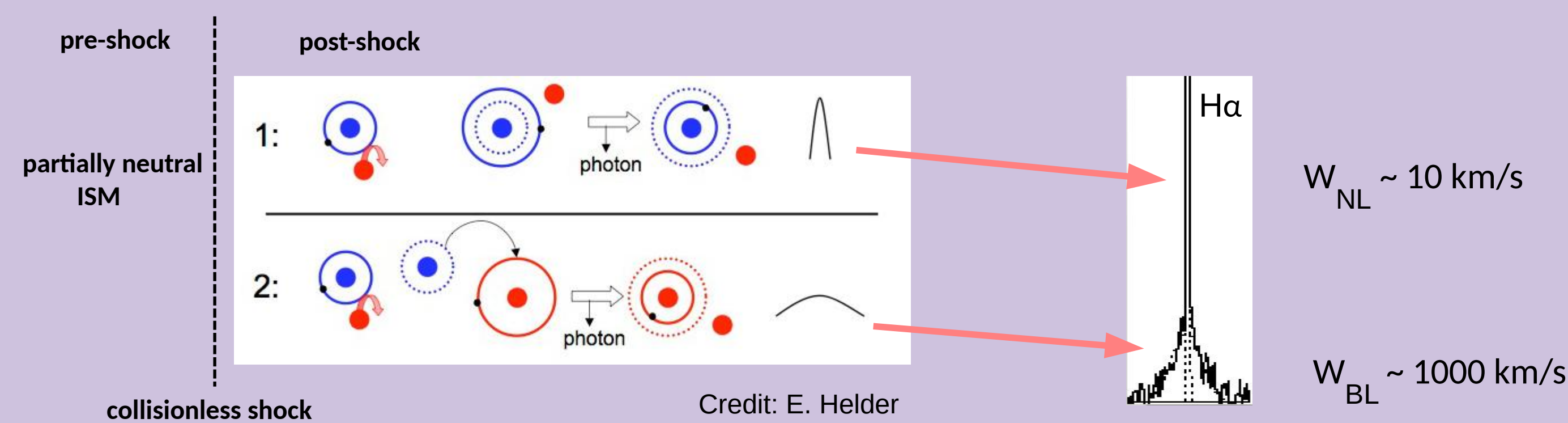
⁴ Harvard-Smithsonian CfA, Cambridge, USA; ⁵ Department of Astrophysics, University of Vienna, Austria.

ABSTRACT

We analyzed MUSE/VLT spectroscopic observations of the supernova remnant SNR 0509-67.5 within the Large Magellanic Cloud. Our primary investigation centered on examining the radial and azimuthal H α -emission profiles. Our findings indicate that the observed radial trends in the broad-component parameters within the northeastern region align with a spherical thin-layer geometric model characterized by high neutral density gradients. However, the shock velocity appears to be lower than what proper motions suggest. Additionally, our analysis reveals that the measured broad-component widths in various locations surrounding the remnant necessitate an understanding of cosmic-ray physics for explanation.

INTRODUCTION

Collisionless shocks traveling through a partially neutral interstellar medium (ISM) exhibit a distinct spectral signature characterized by Balmer lines, and are referred to as **Balmer-dominated shocks**. The H α line is the brightest and its distinctive double-component profile reveals the conditions in both the ISM and the shock. Post-shock protons interact with pre-shock neutrals overtaken by the shock in two ways, resulting in the production of the narrow and broad-line components.



1: Narrow line (NL): produced by cold neutrals (blue circles) from the pre-shock ambient ISM that are collisionally excited by electrons and protons in the shock.

2: Broad line (BL): produced by post-shock hot neutrals (broad neutrals), created through charge exchange between incoming neutrals and hot protons in the shock (red circle).

The width of the broad component can be used to infer the shock acceleration efficiency, while the width of the narrow component and the narrow-to-broad intensity ratio provide the information on the maximum energy of accelerated particles and the amount of cosmic ray (CR) heating in the shock precursor (Blasi et al. 2012, Morlino et al. 2012, Morlino et al. 2013). SNR 0509-67.5 in the Large Magellanic Cloud (LMC) is the best candidate to study CR acceleration (Smith et al. 1994, Helder et al. 2010) since the distance to the LMC is well known and from proper motion studies (Hovey et al. 2015, Arunachalam et al. 2022) we get an independent shock speed estimation of 6270 ± 40 km/s on average.

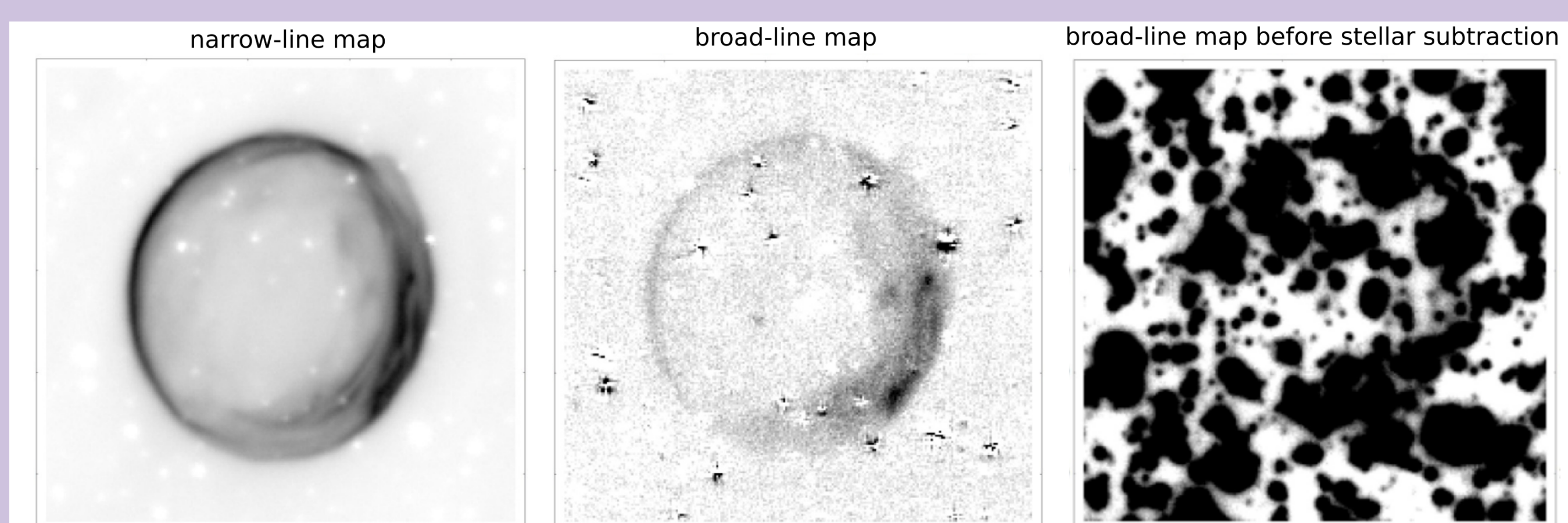
OBSERVATIONS AND DATA REDUCTION

We present observations (0101.D-0151[A] PI Giovanni Morlino) with the Multi Unit Spectroscopic Explorer (MUSE) instrument at the ESO Very Large Telescope. The total integration time was **3 hours** and seeing $\sim 1''$.

MUSE instrument characteristics:

- field-of-view (FOV) of $1' \times 1'$ covers the entire SNR 0509-67.5 (diameter $\approx 30''$);
- spatial scale of $0.2''/\text{pixel}$ enables the tracing of shock filaments and the resolution of geometric effects;
- spectral coverage $4750 - 9350 \text{ \AA}$, spectral resolution $\sim 100 \text{ km/s}$ (only broad component resolved);
- Instrument **high sensitivity** allows for the detection of a very faint broad component in the northeastern (NE) rim.

The data were reduced using the MUSE pipeline recipes version 2.4.2 following the standard reduction procedure. We developed a sky model using regions free from the remnant (including its interior) and stellar emission, and further sampled this region to ensure that only the faintest parts were utilized by the pipeline for sky model estimation.

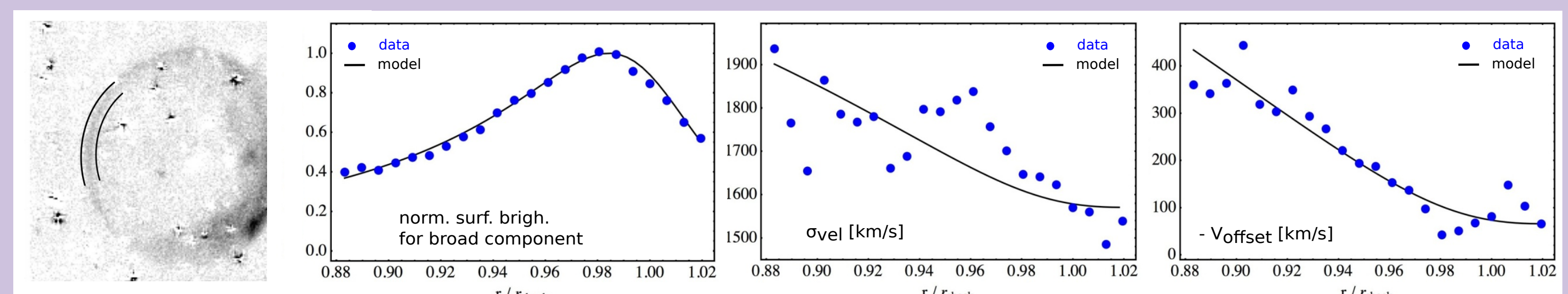


The entire FOV is crowded with stars affecting the observed H α -line profiles at some locations on the remnant. We developed the **stellar subtraction method** creating two off-line stellar images collapsing the datacube around certain wavelength (velocity) channels; one from -20 000 km/s to -8000 km/s and the other from 8000 km/s to 20 000 km/s (the narrow H α component is centered at zero velocity). The selected ranges avoid contamination from the broad H α component, and we minimize biases from the remnant's emission by masking out all pixels within the area occupied by the SNR. Every datacube channel was then fitted with a linear combination of the two stellar images plus a constant, where χ^2 minimization was done over all unmasked pixels. Coefficients of stellar images contribution were smoothed by a second-order polynomial fits applied to their wavelength trends excluding 20% of the coefficients deviating the most from the fits.

RESULTS

Radial profiles

The geometry of the NE rim shows an almost perfect spherical symmetry. We extracted line profiles from $0.2''$ wide circular arcs in the region with position angle $45^\circ - 105^\circ$ and distance from the remnant's center in the range $13.6'' - 15.7''$. We fit double-Gaussian profiles to the H α lines and extract surface brightness, width of the broad component, and its offset with respect to the narrow-component centroid.

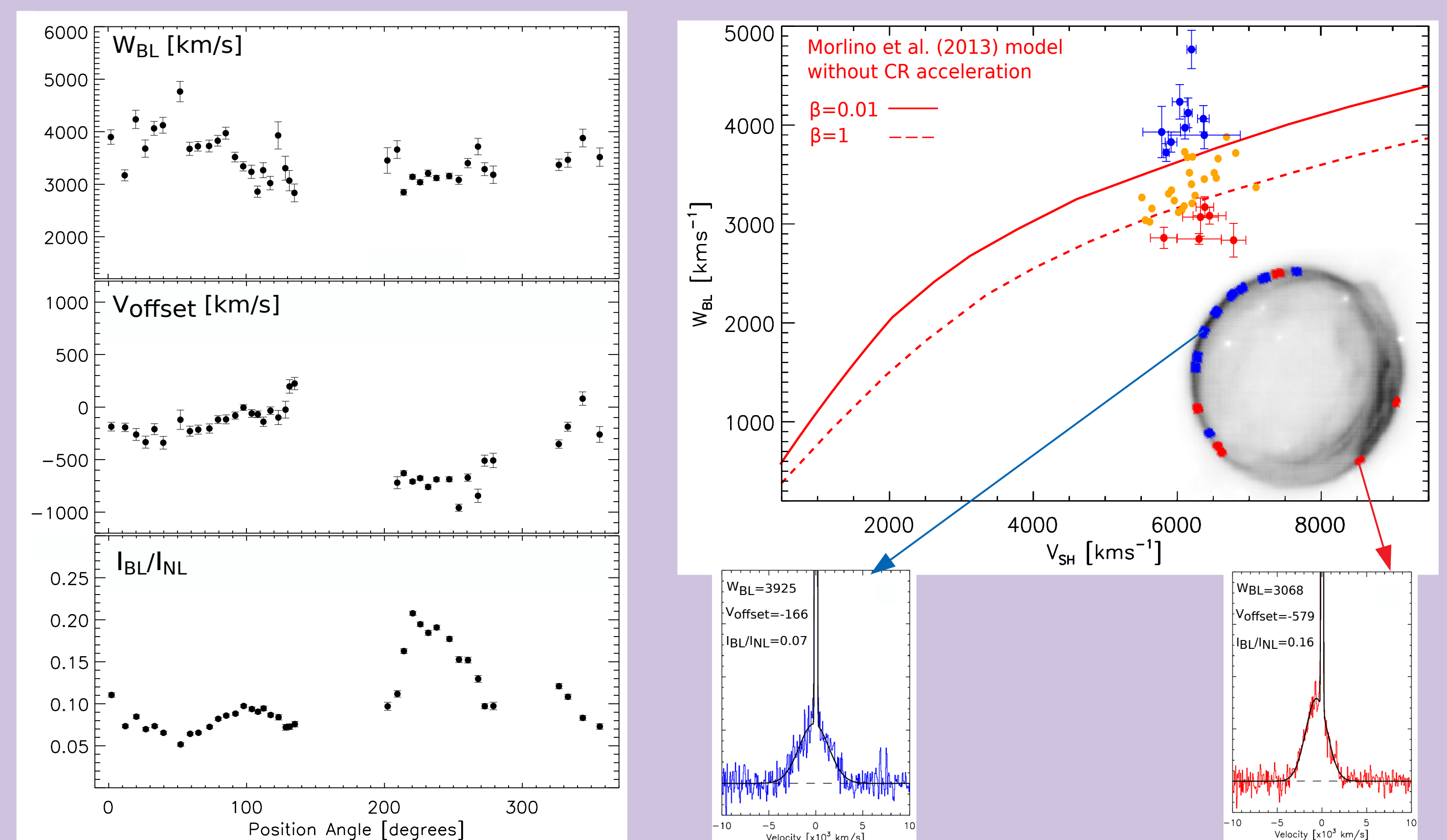


The **geometric model** used to explain the radial profiles of the observables: the emission is confined to a spherical thin shell located at a radial distance r_{sh} from the remnant's center, the shock velocity is radial, while a gradient is allowed for the neutral density in the ambient medium. The broad-line component is modelled taking into account the thermal velocity dispersion (σ_{vel}) and a bulk velocity (V_{bulk} ; with respect to the narrow line component), for different projected distances from the SNR center.

The best fit solution: $r_{sh} \approx 15.4''$, $\sigma_{vel} \approx 1500 \text{ km/s}$, $V_{bulk} \approx 3000 \text{ km/s}$ a density gradient with components $+6.5r_{sh}^{-1}$ in the projected radial direction and $-0.85r_{sh}^{-1}$ along the line-of-sight. This suggests that a **strong local gradient of neutrals in the NE rim** is present.

Azimuthal profiles

We mapped the H α profiles all around the remnant at the locations for which the proper motion was measured and presented in the paper Hovey et al. (2015). We managed to recover **39 out of 44 Hovey et al. (2015) locations** (other segments were significantly affected by a nearby star or signal-to-noise was very low to resolve broad component). We show the azimuthal variation of W_{BL} , V_{offset} , I_{BL}/I_{NL} , and compare the Morlino et al. (2013) shock model predictions without CR acceleration for different electron-to-proton equilibration levels (β). We used the average speed estimates from Arunachalam et al. (2022). The points between the two red lines can be explained without invoking presence of CRs, the **points below the $\beta=1$ line can be understood invoking efficient CR acceleration**.



SUMMARY

- The shock geometry in the NE region indicates that spherical thin layer model with high neutral density gradients can account for the observed radial trends in the broad-component parameters, but with a lower shock velocity ($\approx 4000 \text{ km/s}$) than suggested from proper motions. The smaller speed might be a consequence of the velocity dependence on charge-exchange processes so that the mean velocity of broad neutrals may be significantly different from that of the ions.
- We find the locations around the remnant that need CR physics to be explained. In addition, in some regions we find electron-proton equilibration smaller than 0.01. We plan to quantify the acceleration efficiency where $\beta > 1$ and also examine the cause of $\beta < 0.01$.

References

- [1] Arunachalam, P., Hughes, J. P., Hovey, L., Eriksen, K.: 2022, ApJ, 938, 121
- [2] Blasi, P., Morlino, G., Bandiera, R., Amato, E., Caprioli, D.: 2012, ApJ, 755, 121
- [3] Helder, E. A., Kosenko, D., Vink, J.: 2010, ApJ, 719, L140
- [4] Hovey, L., Hughes, J. P., Eriksen, K.: 2015, ApJ, 809, 119
- [5] Morlino, G., Bandiera, R., Blasi, P., Amato, E.: 2012, ApJ, 760, 137
- [6] Morlino, G., Blasi, P., Bandiera, R., Amato, E., Caprioli, D.: 2013, ApJ, 100, 50
- [7] Smith, R. C., Raymond, J. C., Laming, J. M.: 1994, ApJ, 420, 286